Stem Cell Research 24 (2017) 118–127

Contents lists available at ScienceDirect

Stem Cell Research

journal homepage: www.elsevier.com/locate/scr

Laminin α5 substrates promote survival, network formation and functional development of human pluripotent stem cell-derived neurons *in vitro*

Anu Hyysalo [a,*], Mervi Ristola [a], Meeri E.-L. Mäkinen [a], Sergei Häyrynen [b], Matti Nykter [b], Susanna Narkilahti [a]

[a] NeuroGroup, BioMediTech, University of Tampere, Lääkärinkatu 1, 33520 Tampere, Finland
[b] Computational Biology, BioMediTech, University of Tampere, Lääkärinkatu 1, 33520 Tampere, Finland

ARTICLE INFO

Article history:
Received 7 December 2016
Received in revised form 28 August 2017
Accepted 7 September 2017
Available online 12 September 2017

Keywords:
Alpha5 laminin substrate
Human pluripotent stem cell-derived neuron
In vitro culturing
Microelectrode array
Neuronal networks

ABSTRACT

Laminins are one of the major protein groups in the extracellular matrix (ECM) and specific laminin isoforms are crucial for neuronal functions in the central nervous system *in vivo*. In the present study, we compared recombinant human laminin isoforms (LN211, LN332, LN411, LN511, and LN521) and laminin isoform fragment (LN511-E8) in *in vitro* cultures of human pluripotent stem cell (hPSC)-derived neurons. We showed that laminin substrates containing the α5-chain are important for neuronal attachment, viability and network formation, as detected by phase contrast imaging, viability staining, and immunocytochemistry. Gene expression analysis showed that the molecular mechanisms involved in the preference of hPSC-derived neurons for specific laminin isoforms could be related to ECM remodeling and cell adhesion. Importantly, the microelectrode array analysis revealed the widest distribution of electrophysiologically active neurons on laminin α5 substrates, indicating most efficient development of neuronal network functionality. This study shows that specific laminin α5 substrates provide a controlled *in vitro* culture environment for hPSC-derived neurons. These substrates can be utilized not only to enhance the production of functional hPSC-derived neurons for *in vitro* applications like disease modeling, toxicological studies, and drug discovery, but also for the production of clinical grade hPSC-derived cells for regenerative medicine applications.

1. Introduction

Laminins, one of the major protein groups in the extracellular matrix (ECM), play an important role in the central nervous system (CNS) (Barros et al., 2011). Laminins are large heterotrimeric glycoproteins consisting of α, β and γ chains, which assemble into cross-shaped molecules. To date, 5 α, 3 β, and 3 γ chains have been identified and associate to form at least 15 different laminin isoforms (Indyk et al., 2003). Laminins are involved in many aspects of CNS physiology and neuronal functions, but their exact biological roles in the formation, development, and function of neuronal networks remain largely unknown (Domogatskaya et al., 2012).

Information regarding expression and function of specific laminin chains or isoforms in different CNS regions has mainly been collected from gene expression and inactivation studies in animal models and studies of human laminin diseases. Extensive mRNA sequencing has revealed the expression of several laminin chains (α1, α3, α4, α5, β1, β2, γ1) in the fetal human and embryonic mouse ventricular zone, subventricular zone and cortical plate, but the biological significance of these chains was not evaluated (Fietz et al., 2012). Furthermore, the functional role of laminins containing the α5 chain has been shown in neural tube formation and neural crest cell migration during mouse embryogenesis (Coles et al., 2006; Miner et al., 1998). Later in development, laminin (LN) 511 (α5, β1, γ1) has been identified as the major neuronal laminin in the basement membrane of mouse hippocampus (Indyk et al., 2003). In addition, cortical histogenesis, development and pial basement membrane formation are disturbed by mutations in the laminin β2, γ1, and γ3 chains (Barak et al., 2011; Halfter et al., 2002; Radner et al., 2013). LN411 or LN511 and LN111 or LN211, which are produced by endothelial cells and astrocytes, respectively, participate in the formation of the blood-brain barrier (Sixt et al., 2001), and laminins containing the α2 chain are required for oligodendrocyte maturation and CNS myelination in mice (Chun et al., 2003). Thus, although several laminin chains or isoforms have been identified in the CNS, knowledge regarding the overall expression and functions of laminins is not comprehensive.

Studying laminin isoforms *in vivo* is challenging due to the overlapping functions of laminin chains and isoforms (Simon-Assmann et al.,

Abbreviations: hPSC, human pluripotent stem cell; LN, laminin; MEA, microelectrode array.

* Corresponding author at: Institute of Biosciences and Medical Technology (BioMediTech), University of Tampere, Lääkärinkatu 1, 33520 Tampere, Finland.
E-mail address: anu.hyysalo@staff.uta.fi (A. Hyysalo).

http://dx.doi.org/10.1016/j.scr.2017.09.002

2011). However, the production of reliably purified and commercially available laminin isoforms has enabled more detailed *in vitro* experiments to be performed to examine the roles of specific laminin isoforms. Chemically defined, xeno-free, recombinant laminin isoforms that are suitable for clinical use have been marketed for a few years. *In vitro* studies with mouse dorsal root ganglion neurons have shown that LN111 and LN511 provide superior support for neurite outgrowth compared to LN211 and LN411 (Plantman et al., 2008). LN511 also remarkably promotes the elongation of axons and dendrites of rat hippocampal neurons compared to LN111, LN211 and LN411 (Fusaoka-Nishioka et al., 2011). Furthermore, the E8 fragment of LN511 promotes axon and dendrite outgrowth and increases the number of dendrites in rat hippocampal neurons (Fusaoka-Nishioka et al., 2011). However, the results obtained with murine neurons cannot be directly translated to human neurons.

Human pluripotent stem cells (hPSCs) are considered as an excellent tool for research and clinical purposes. Previously, LN111, LN332, LN511, LN521, and the E8 fragment of LN511 have been shown to efficiently support the self-renewal of hPSCs (Lu et al., 2014; Miyazaki et al., 2008; Miyazaki et al., 2012a; Rodin et al., 2010). Currently, only a few studies addressing the use of specific laminin isoforms or fragments and differentiating hPSC-derived neurons have been published. Dopaminergic neurons were produced from human induced pluripotent stem cells (hIPSCs) under xeno-free conditions using LN521 or the E8 fragment of LN511 (Doi et al., 2014; Lu et al., 2014; Nakagawa et al., 2014).

In addition to the morphological and biochemical characterization, it is crucial to assess the functionality of neuronal networks *in vitro*. Despite the importance of this aspect, it has barely been addressed in previous laminin studies. Neuronal network functionality and development *in vitro* can be exclusively evaluated using microelectrode array (MEA) technology, as previously shown for hPSC-derived neurons (Heikkilä et al., 2009; Yla-Outinen et al., 2010). In this study, we compared the recombinant human laminin isoforms LN211, LN411, LN332, LN511, and LN521, as well as the LN511-E8 fragment as substrates for hPSC-derived neuronal cultures. To our knowledge, this is the first publication to report the effects of different laminin isoforms as *in vitro* coating substrates on neuronal network activity.

2. Materials and methods

2.1. Neuronal differentiation and laminins

The human embryonic stem cell (hESC) line Regea 08/023, derived and characterized at the Institute of Biosciences and Medical Technology (BioMediTech, University of Tampere, Finland) (Skottman, 2010), was used. An additional hESC line (Regea 11/013; (Skottman, 2010)) and hIPSC line (04511WTs; (Ojala et al., 2016)) were studied with less extensive analyses to confirm the obtained results. Neurons were differentiated in suspension cultures, as previously described (Lappalainen et al., 2010). For neuronal maturation and comparison of the cell behaviors on different laminin substrates, predifferentiated cells were plated on polystyrene or MEA (Axion Biosystems, Atlanta, GA, USA) coated with the human recombinant laminins LN211, LN332, LN411, LN511, LN521 (2 μg/cm^2, BioLamina, Sundbyberg, Sweden), or the LN511-E8 fragment (iMatrix-511, 1 μg/cm^2, Clontech, Takara Bio Inc., Shiga, Japan). Chain compositions of the laminins used in this study are listed in Supplementary Table 1. Laminin from Engelbreth-Holm-Swarm murine sarcoma basement membranes (2 μg/cm^2, Sigma-Aldrich, St. Louis, MO, USA) and laminin from human placenta (2 μg/cm^2, Sigma Aldrich) were used as control coating substrates, as we have routinely used these substances for hPSC-derived neurons (Lappalainen et al., 2010; Toivonen et al., 2013). Morphology of the cells on different laminin substrates was evaluated using phase contrast imaging.

2.2. Cell viability and spreading analysis

Viability and spreading of neurons cultured on laminin substrates for one week were investigated using an automated cell counter (Countess®, Thermo Fisher Scientific) or a LIVE/DEAD® Viability/Cytotoxicity Kit for mammalian cells (Thermo Fisher Scientific) as previously described (Ylä-Outinen et al., 2014).

2.3. Immunocytochemistry

Immunocytochemical characterization was performed to investigate neuronal protein expression, as previously described (Lappalainen et al., 2010). Neurons cultured on laminin substrates for one week were fixed and stained with mouse anti-SRY (sex determining region Y)-box 2 (SOX2; 1:200, R&D systems Inc., Minneapolis, MN, USA), rabbit anti-microtubule-associated protein (MAP-2, 1:400; Merck Millipore), rabbit anti-β-tubulin isotype III (1:2000; GenScript, Piscataway, NJ, USA), and chicken anti-glial fibrillary acidic protein (GFAP; 1:4000, Abcam, Cambridge, UK). For secondary antibody labeling, Alexa Fluor 488- (1:400) and Alexa Fluor 568-conjugated antibodies (1:400) (both from Thermo Fisher Scientific) were used.

2.4. Gene expression analysis

Total RNA was extracted from neurons cultured for one week on laminin isoforms using a NucleoSpin RNA XS kit (Macherey-Nagel, Düren, Germany). The concentration and quality of the RNA were spectroscopically monitored. RNA was reverse transcribed into cDNA using the High Capacity cDNA Reverse Transcription kit (Applied Biosystems, Thermo Fisher Scientific). Eighty-four genes of interest were analyzed using a commercial TaqMan® Array for Human Extracellular Matrix & Adhesion Molecules (Applied Biosystems, Thermo Fisher Scientific). Furthermore, a subset of these genes were also analyzed using TaqMan® Gene Expression Assays.

2.5. Microelectrode array

The spontaneous electrical activity of the neuronal networks generated on different laminin substrates was measured using standard 12-well plate MEAs, the Maestro MEA system, and AxIS software (all from Axion Biosystems). Ten minute recordings were performed once a week for a minimum of three weeks. Spike counts and burst analyses were performed using a custom-made MATLAB script (Kapucu et al., 2012), with further modifications.

More detailed description of the Materials and methods are provided in the Supporting information.

3. Results

3.1. LN511 efficiently supports network formation and viability of hPSC-derived neurons

In this study, hPSC -derived neurons were cultured on the recombinant human laminin isoforms LN211, LN332, LN411 and LN511. Previously, the expression of specific chains from all these isoforms in the CNS has been reported (Fietz et al., 2012). Cell morphology and network formation was visually assessed from phase contrast images. The hPSC-derived neurons attached most efficiently and formed networks with the highest density and most even distribution on LN511 (Fig. 1A). The behavior of cells on LN511 was visually similar to cells on mouse laminin. Fewer cells attached to LN411 compared to the other laminin isoforms, and instead of forming a network, the viable cells aggregated. The behavior of cells cultured on LN411 resembled the cultures on human laminin. Cell attachment and neuronal network formation on the LN211 and LN332 isoforms were more efficient than on LN411 but lesser than in cultures on LN511 and mouse laminin.

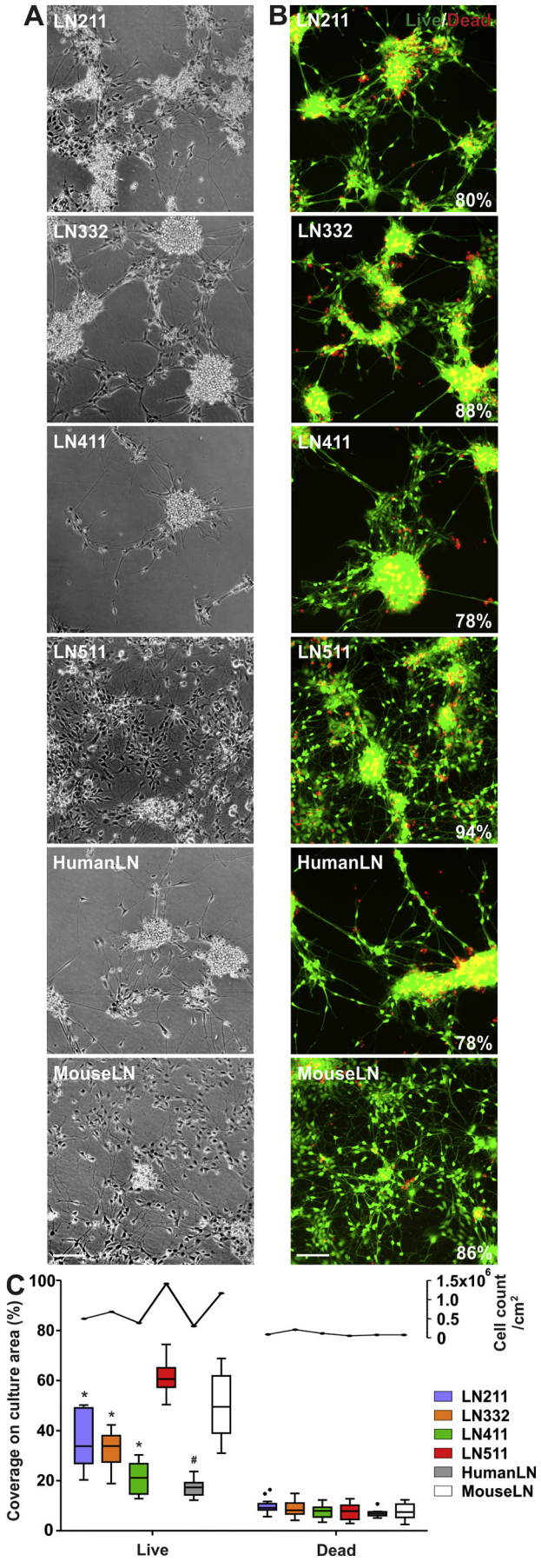

Cell viability and the amounts of live and dead cells were quantified with automated cell counter. In addition, spreading of the viable cells in the cultures was determined with live/dead staining and quantified as the percentage of culture area covered with cells positive for live or dead staining. The highest cell viability (median [mdn] 94%, $p \leq 0.045$) and live cell count (mdn 1.42 $\times$ 10^6 cells/cm^2) were detected on LN511 (Fig. 1B–C). Similar result was obtained from analysis of live cell coverage, as live cell coverage was significantly lower in cultures on the other laminin isoforms compared to cultures on LN511 (mdn_{LN511} 61%, all $p < 0.01$) and mouse laminin ($mdn_{mouse\ laminin}$ 50%, all $p < 0.03$). Cell viability on other substrates, ranged from 78% (LN411 and human laminin) to 88% (LN332). The amounts of live cells and live cell coverages, however, demonstrated differences between the cultures more clearly. The live cell counts detected on LN211 and LN332 were 0.50 and 0.68 $\times$ 10^6 cells/cm^2, respectively, whereas the live cell coverage on both substrates was 34%. The lowest live cell counts (mdn 0.39 and 0.31 $\times$ 10^6 cells/cm^2) and live cell coverages (mdn 21% and 17%) were observed in cultures on LN411 and human laminin. Similar levels of dead cell coverage and dead cell counts were detected on every substrate.

3.2. The largest number of hPSC-derived neurons is detected on LN511

Total cell counts and the number of cells positive for the neuronal markers MAP-2 and β-tubulin$_{III}$ were quantified to confirm the neuronal identity of the differentiated cells on the laminin isoforms. The majority of the cells in all cultures were stained with MAP-2 and β-tubulin$_{III}$ and few GFAP-positive astrocytes were found, regardless of the coating substrate. Neural precursor cells in the cultures were detected with SOX2. Representative images of cells stained for MAP-2, β-tubulin$_{III}$, and GFAP are presented in Fig. 2A.

The highest total cell (mdn 1610 cells/image) and neuron (mdn 1173 neurons/image) counts were detected in cultures on LN511 (Fig. 2B–C). The total cell count was only significantly increased on LN511 ($p < 0.01$) compared to mouse laminin (mdn 1112 cells/image) (Fig. 2B). The neuron count on LN511 was also higher but not significantly different ($p = 0.08$) from mouse laminin (mdn 799 neurons/image) (Fig. 2C). Both cell counts were significantly increased on LN511 compared to all other laminin isoforms (total cell count, all; $p < 0.01$) (neuron count, LN211 [$p < 0.01$], LN332 [$p = 0.05$], LN411 [$p < 0.01$]) (Fig. 2B–C). The neuron percentage (neuron count/total cell count) in the cultures varied between 59% (LN411) and 80% (LN211). Most of the remaining population expressed SOX2, while some SOX2-positive cells also expressed MAP-2 and β-tubulin$_{III}$ (Supplemental Fig. 1).

The hESC line Regea 11/013 and hIPSC line 04511WTs were used and analyzed in terms of cell attachment and morphology, and protein expression to confirm that the results obtained with hESC line Regea 08/023 are independent of the used cell line. Similar differences between the laminin isoforms were detected with both cell lines, supporting our results with Regea 08/023 cells (Supplemental Fig. 2). Taken together, the immunocytochemical analysis confirmed that the LN511 isoform most efficiently supported the formation of dense and

Fig. 1. Cell morphology and live/dead analysis of hPSC-derived neurons on different laminin isoforms. The hPSC-derived neurons were cultured on LN211, LN332, LN411, LN511, mouse laminin and human laminin for one week. A) Representative phase contrast images of the neuronal networks formed on different laminin isoforms. Scale bar: 100 μm. B) Representative images of live/dead-stained cells on different laminin isoforms presented with median cell viability percentage on each culture substrate. Scale bar: 100 μm. C) Quantification of cell spreading (live/dead cell coverage) and live and dead cell counts in the cultures. The cell spreading quantification data from three biological experiments are presented as Tukey boxplots on the left y-axis. Mann-Whitney *U*-test (*$p \leq 0.05$ compared to LN511 and mouse laminin; #$p \leq 0.05$ compared to mouse laminin). All isoforms and human laminin were first compared pairwise with mouse laminin. Furthermore, LN211, LN332 and LN411 were then compared pairwise with LN511. The corresponding live and dead cell counts for each culture substrate are presented as median values on the right y-axis.

viable neuronal networks, whereas LN411 and human laminin provided the least support.

3.3. Gene expression profiles of ECM-associated molecules in neurons cultured on different laminin isoforms

The expression profiles of 84 genes in neurons cultured on different laminin isoforms were compared. Fourteen of these genes were excluded from the analyses due to their considerably low or undetected expression. In general, the expression of several genes related to human ECM and cell adhesion were upregulated compared to suspension samples (Fig. 3A). The majority of the studied genes were expressed at lower levels in neurons cultured on LN411 than on the other laminin isoforms and mouse laminin. The gene expression profile of cells cultured on LN411 mainly resembled cells cultured on human laminin.

Based on the results from this study showing that neuron attachment, viability and network formation are the most efficient on LN511 and least successful on LN411, the gene expression profiles between neurons cultured on these substrates were compared in more detail. Fifteen genes with either a minimum of a three-fold difference in relative expression or statistically significant differences between cultures on LN511 and LN411 were identified (Fig. 3B). Seven of these genes encoded ECM proteins (*COL1A1*, *COL8A1*, *COL11A1*, *COL15A1*, *LAMB3*, *ECM1*, and *FN1*). Several α1 chains from different collagens (*COL1A1* 3.5-, *COL8A1* 10.6-, *COL11A1* 2.4- [$p = 0.04$], *COL15A1* 3.3-fold, respectively) were considerably upregulated in cells cultured on LN511 compared to the cultures on LN411. Laminin β3-chain (*LAMB3*) was upregulated 11.1-fold in the cultures on LN511. Additional ECM proteins that are not included in the laminin or collagen families, extracellular matrix protein 1 (*ECM1*) and fibronectin (*FN1*), were upregulated 4.6- and 4.4-fold, respectively, in cells cultured on LN511.

Considerable differences in the relative expression levels of several cell surface adhesion molecules were also detected between cells cultured on LN511 and LN411 (Fig. 3B). Three integrin subunits, α1, αV, and β4 (*ITGA1*, *ITGAV*, and *ITGB4*) were upregulated 3.3-, 1.7- ($p = 0.04$), and 3.1-fold, respectively, and intercellular adhesion molecule 1 (*ICAM1*) was significantly upregulated in cells cultured on LN511 (12.7-fold, $p = 0.01$). Two different proteases, matrix metalloproteinase 10 (*MMP10*) and a disintegrin and metalloproteinase with a thrombospondin type 1 motif, member 13 (*ADAMTS13*), were upregulated 4.6-fold and downregulated 1.2-fold ($p = 0.004$), respectively, in cultures on LN511. Connective tissue growth factor (*CTGF*) and transforming growth factor, beta-induced ECM protein (*TGFBI*) were both significantly upregulated in cells cultured on LN511 (3.0-fold ($p = 0.045$) and 8.0-fold ($p = 0.04$), respectively).

Similar trend in gene expression levels between cells cultured on LN511 and LN411 was observed with Regea 11/013 and 04511WTs –derived cells. The most distinctive differences between LN511 and LN411 cultures within all studied cell lines were detected as upregulation of *ICAM1* and *TGFBI* in cells cultured on LN511 (Supplemental Fig. 3). In summary, considerable differences were discovered in the expression profiles for genes encoding ECM proteins, cell surface adhesion molecules, proteases, and growth factors, and majority of these genes were upregulated in cultures on LN511 compared to cultures on LN411.

3.4. Widest distribution of electrophysiologically active neurons is detected on LN511

MEA technology was used to evaluate the functionality of the neuronal networks generated on different laminin isoforms. Electrophysiological activity was assessed using the following parameters: proportion of spike-detecting electrodes; spontaneous spiking frequency in active electrodes; proportion of burst-detecting electrodes of all electrodes; and total burst counts in the burst-detecting electrodes.

The neuronal network density and cell morphology were evaluated during the MEA experiments using phase contrast microscopy. Cell

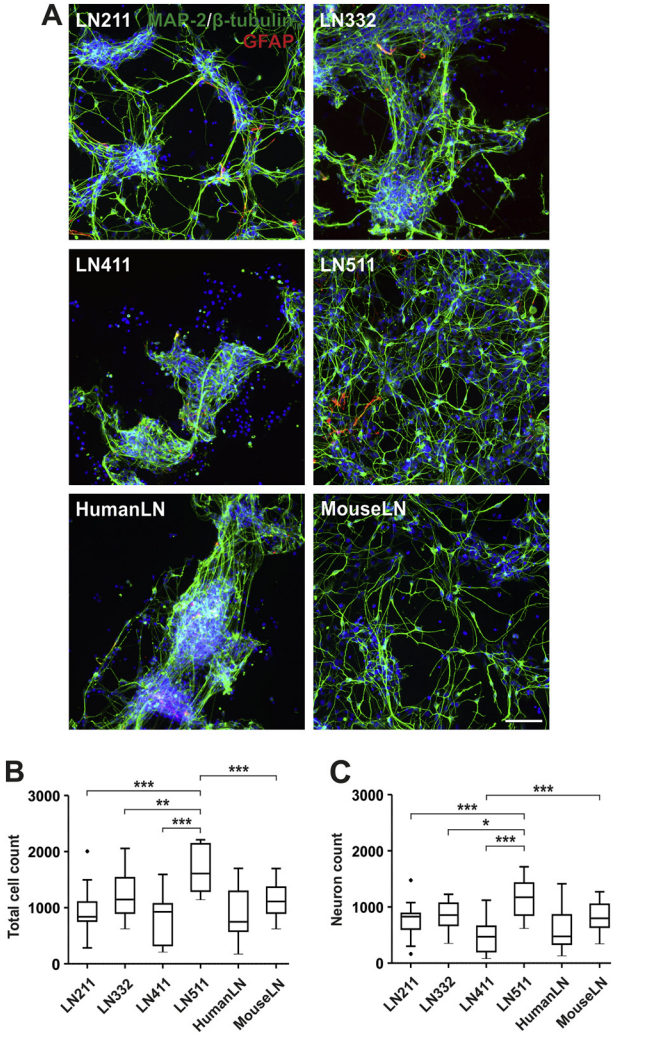

Fig. 2. Immunocytochemical characterization of hPSC-derived neurons on different laminin isoforms. Protein expression of the neuronal markers MAP-2 and β-tubulin$_{III}$ were determined in hPSC-derived neurons cultured on LN211, LN332, LN411, LN511, mouse laminin and human laminin for one week. A) Representative images of MAP-2/β-tubulin$_{III}$/GFAP-stained cells on different laminin isoforms. Scale bar: 100 μm. B) Total cell counts and C) neuron counts were quantified in cultures on LN211, LN332, LN411, LN511, mouse laminin and human laminin after one week. Partial cell detachment was detected on LN411, LN332, and human laminin during immunocytochemistry, which may have affected the results of the quantification. The data from three biological experiments presented as Tukey boxplots. Mann-Whitney *U* test ($^{*}p \le 0.05$; $^{**}p \le 0.01$; $^{***}p \le 0.005$). All isoforms and human laminin were first compared pairwise with mouse laminin. Furthermore, LN211, LN332 and LN411 were then compared pairwise with LN511.

attachment, morphology, and network formation on MEAs coated with different laminin isoforms were similar to the results described above, detected on polystyrene. The attached cells proliferated on all coating substrates, but the initial differences in network density also remained at later time points (Supplemental Fig. 4).

Cells formed spontaneously active neuronal networks on all tested substrates and showed both spike and burst activity (Fig. 4A–B). The highest percentages of spike- and burst-detecting electrodes were observed on LN511 at every time point. The percentages of spike- and burst-detecting electrodes on LN511 increased from 14% to 33% and from 5% to 11%, respectively, over time. The active electrode levels were significantly reduced in cultures on LN211 compared to LN511 at one and two weeks, but at three weeks, no significant differences were detected (Fig. 4A–B). On LN211, the active electrode levels were similar to the cultures on mouse laminin. Cultures on LN332 and LN411 showed the lowest levels of spike- and burst-detecting

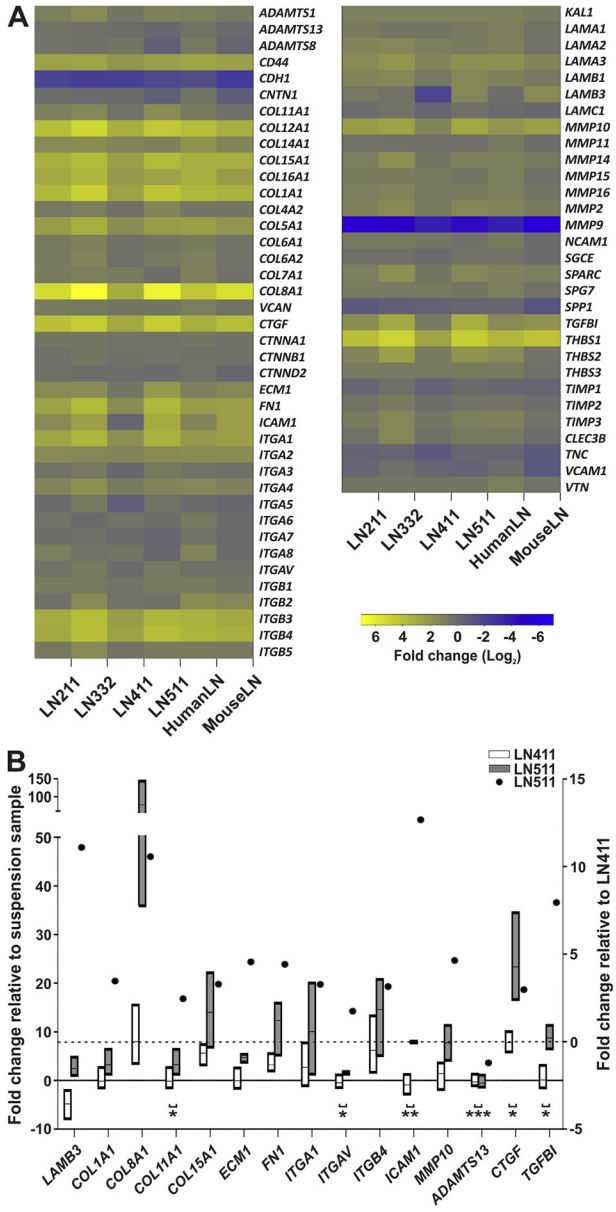

Fig. 3. Relative changes in gene expression in hPSC-derived neurons on different laminin isoforms. The expression profiles of genes encoding for human ECM and adhesion molecules were examined in hPSC-derived neurons cultured on LN211, LN332, LN411, LN511, mouse laminin and human laminin for one week. A) The mean fold changes relative to the suspension sample are presented as a heatmap in the $\log_2$ scale. B) The mean fold changes in the expression, relative to suspension sample, of genes with either statistically significant differences or a minimum of a three-fold difference in relative expression between cells cultured on LN411 and LN511 are presented as floating bars (min-max) on the left y-axis. Student's *t*-test (*$p \le 0.05$; **$p \le 0.01$; ***$p \le 0.005$). Furthermore, the mean fold changes in cells cultured on LN511 relative to cells cultured on LN411 are presented as dots on the right y-axis. The data from three biological experiments are presented.

electrodes (range LN332[spike] 1–10%; LN332[burst] 0–3%; LN411[spike] 2–6%; and LN411[burst] 0–1%). Compared to the cultures on LN511, the active electrode counts were significantly reduced on both these substrates at every time point, excluding the burst-detecting electrode level on LN411 at one week (Fig. 4A–B). The active electrode levels on LN332 and LN411 were similar to cultures on human laminin. In general, the relative amounts of spike- and burst-detecting electrodes developed similar trends in all cultures, and the highest activity was detected at the three week time point.

Increased spiking frequency and bursting activity are considered as a sign of functional maturation in cultured neuronal networks (Wagenaar et al., 2006). A slight increasing trend in spontaneous spiking frequency was detected in all cultures over time (Fig. 4C). For example, cells grown on mouse laminin presented median spiking frequencies of 0.10, 0.12, and 0.13 Hz at one, two, and three weeks, respectively. When the spiking frequencies in cultures on each laminin isoform were compared to cultures on LN511 and mouse laminin, few significant differences were observed at one and two weeks, but no differences were observed at the three week time point. Cells on LN332 showed a significantly lower spiking frequency (0.06 Hz) than on LN511 (0.10 Hz) or mouse laminin (0.10 Hz) at one week ($p[LN511] < 0.01$, $p[mouse\ LN] = 0.01$). The spiking frequency of cells cultured on LN411 (0.10 Hz) was significantly reduced at two weeks compared to cells cultured on LN511 (0.21 Hz) ($p < 0.01$). The total burst counts in burst-detecting electrodes were not affected by the coating substrate or time (Fig. 4D). The only significant difference was observed between cells cultured on LN211 (2.9 bursts/min) and mouse laminin (1.5 bursts/min) at the three week time point.

In conclusion, the neuronal networks generated on LN511 contain the widest distribution of functional neurons. Spike or burst frequencies in active electrodes were clearly not affected by the substrate.

3.5. All laminin α5 substrates support attachment and network formation of hPSC-derived neurons

In this study, we have shown that LN511 efficiently supports cell viability, network formation, and the growth of hPSC-derived neurons. We demonstrated the importance of the laminin α5-chain in *in vitro* cultures of hPSC-derived neurons. Other commercially available substrates, LN521 containing the α5-chain and the LN511-E8 fragment containing the C-terminal region of the α5-chain (Fig. 5A), were studied next. These specific laminin substrates have been used for *in vitro* cultures of hPSCs (Miyazaki et al., 2012b; Rodin et al., 2014a), but a comparison of hPSC-derived neurons has not been performed.

Here, hPSC-derived neurons were cultured on LN511-E8, LN521, LN511 and mouse laminin. Cell attachment, morphology, and network formation were similar on all substrates, as detected by phase contrast microscopy (Fig. 5B). Representative images of immunostained cells on different substrates are presented in Fig. 5C. The total cell counts and number of MAP-2- and β-tubulinIII-positive cells were quantified as described above. The highest total cell count was detected on LN511 (mdn 1287 cells/image), but the approximately same total cell count was observed on LN521 (mdn 1264 cells/image) (Fig. 5D). The total cell counts on LN511-E8 and mouse laminin were lower, but not significantly different (mdn 998 and 930 cells/image, respectively), compared to cultures on LN511 and LN521. A similar trend was detected when the neuron counts were compared in different cultures. Neuron counts on LN511 (mdn 896 neurons/image) was significantly higher compared to cultures on LN511-E8 (603 neurons/image, $p < 0.005$) and mouse laminin (585 neurons/image, $p < 0.01$) (Fig. 5E). However, the proportion of neurons was similar in all cultures, ranging from 76% (mouse laminin) to 71% (LN511).

3.6. Similar development of neuronal network functionality is detected on all laminin α5 substrates

Neuronal network functionality was measured as described above, and spontaneous activity in cultures on LN511-E8 and LN521 was compared to cultures on LN511 and mouse laminin. The behaviors of cells grown on these substrates on MEA was similar to the results described above, detected on polystyrene (Fig. 6A).

Neuronal networks generated on LN511-E8, LN521, and LN511 presented similar trends in the development of activity (Fig. 6B–C), with higher spike- and burst-detecting electrode levels compared to cultures on other substrates (Fig. 4A–B). The highest percentages of active spike- and burst-detecting electrodes were observed in cultures on LN521, with the exception of the burst-detecting electrode levels at one week.

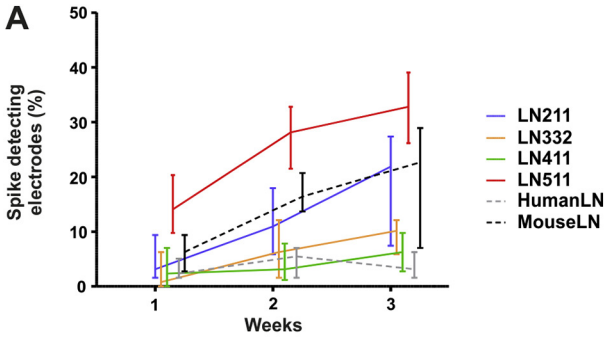

Spike detecting electrodes (%), p-values				
		1 week	2 weeks	3 weeks
MouseLN	LN211	n.s.	n.s.	n.s.
	LN332	n.s.	0.035	n.s.
	LN411	n.s.	0.005	n.s.
	LN511	0.025	n.s.	n.s.
	HumanLN	n.s.	0.01	n.s.
LN511	LN211	n.s.	0.006	n.s.
	LN332	>0.001	>0.001	0.003
	LN411	0.012	>0.001	>0.001

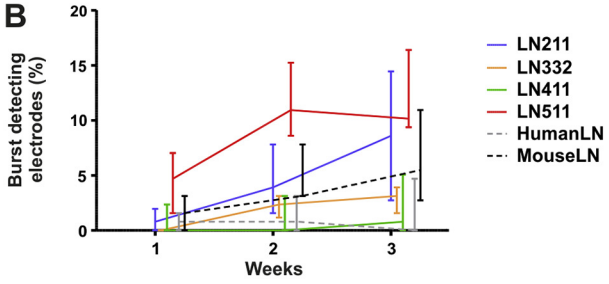

Burst detecting electrodes (%), p-values				
		1 week	2 weeks	3 weeks
MouseLN	LN211	n.s.	n.s.	n.s.
	LN332	n.s.	n.s.	n.s.
	LN411	n.s.	0.025	n.s.
	LN511	n.s.	0.005	n.s.
	HumanLN	n.s.	0.035	n.s.
LN511	LN211	0.048	0.006	n.s.
	LN332	>0.001	>0.001	>0.001
	LN411	n.s.	>0.001	>0.001

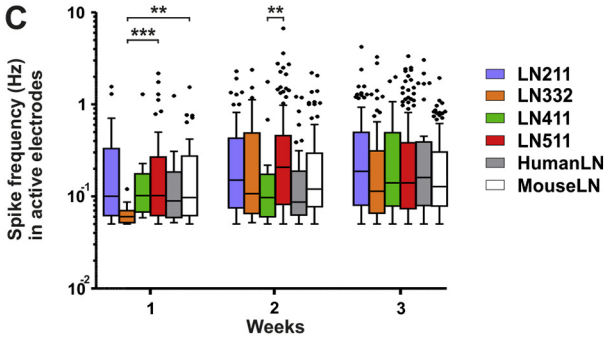

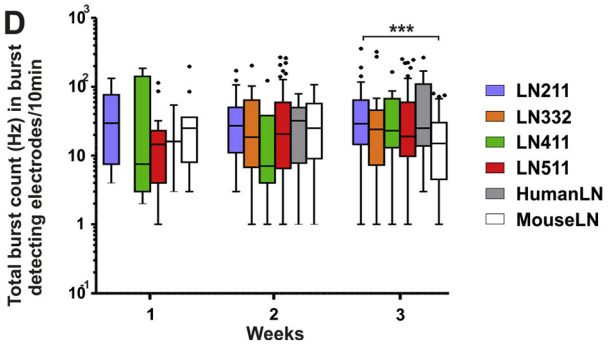

Percentages of spike- and burst-detecting electrodes increased from 10% to 44% and from 0% to 20%, respectively, over time. The lowest percentages of active electrodes were detected on mouse laminin, with the exception of the burst-detecting electrode level at one week. Percentages of spike- and burst-detecting electrodes increased from 4% to 30% and from 1% to 8%, respectively, over time. At the two and three week time points, the spike- (both $p < 0.05$) and burst-detecting ($p < 0.05$, $p < 0.01$ at two and three weeks, respectively) electrode levels in cultures on LN521 were significantly higher than in cultures on mouse laminin. No significant differences in the active electrode levels were detected in cultures on LN521 and LN511-E8 compared to cultures on LN511.

The highest spontaneous spiking frequency in active electrodes was also observed in cultures on LN521 at every time point, ranging from 0.09 Hz to 0.22 Hz (Fig. 6D). The spontaneous spiking frequency increased over time in cultures on every substrate. No significant differences were detected at one or two weeks, but at three weeks, cells cultured on LN521 presented significantly higher spiking frequencies than cells on LN511 (0.14 Hz, $p < 0.05$) or mouse laminin (0.12 Hz, $p < 0.01$) (Fig. 6D). No significant differences were observed in the total burst counts in burst-detecting electrodes between cultures at one or two weeks, but at the three week time point, cells on mouse laminin showed significantly lower burst counts (0.9 bursts/min) than cells on LN511-E8 (2.4 bursts/min, $p = 0.01$) or LN521 (2 bursts/min, $p = 0.03$) (Fig. 6E).

Taken together, the results indicate that on all laminin α5 substrates neurons developed visually indistinguishable networks. The distribution of active neurons in the cultures, as well as spike and burst frequencies, were relatively similar in neurons cultured on LN511-E8 and LN521 compared to cultures on LN511. These results were confirmed with additional hESC line Regea 11/013 and hIPSC line 04511WTs (Supplemental Fig. 5). Although the overall activity of different cell lines was slightly varying, similar pattern of neuronal network activity on laminin α5 substrates was detected with all studied cell lines.

4. Discussion

In this study, we first compared cell attachment, viability and neuronal network formation on LN211, LN332, LN411, and LN511. The hPSC-derived neurons exhibited the most efficient attachment and neuronal networks formation on LN511. The highest cell viability, live cell count, and live cell coverage, indicating efficient spreading of the viable cells in the cultures, were observed in cultures on LN511. The lowest cell attachment and live cell count, with limited network formation, were detected on LN411. Cells on LN211 and LN332 showed moderate cell attachment, live cell count, and network formation. Cell viability percentage was significantly higher on LN511 compared to all other cultures. However, the effect of culture substrate on cell viability percentage is challenging to detect as the detached dead cells are mostly removed from the cultures during media changes. Thus, it was considered that the actual amount of live cells in the cultures better reflected the differences between the culture substrates. The total cell counts analyzed from immunocytochemical images corresponded to the neuron counts on all laminin substrates, indicating that the remaining neural precursor cells in the population did not influence the preference of hPSC-derived

Fig. 4. Development of spontaneous neuronal functionality in cultures on different laminin isoforms. The hPSC-derived neurons were cultured on MEAs coated with LN211, LN332, LN411, LN511, mouse laminin and human laminin for three weeks and electrophysiological activity was measured once a week. A) Percentages of spike-detecting electrodes and B) burst-detecting electrodes in the cultures on different laminin isoforms after one, two, and three weeks. The results are presented as medians with interquartile ranges from three biological experiments. C) Development of the spontaneous spiking frequency in active electrodes and D) total burst counts in the burst-detecting electrodes. The data from three biological experiments presented as Tukey boxplots. Mann-Whitney *U* test (*$p \le 0.05$; **$p \le 0.01$; ***$p \le 0.005$). All isoforms and human laminin were first compared pairwise with mouse laminin. Furthermore, LN211, LN332 and LN411 were then compared pairwise with LN511. Comparisons were performed at every time point.

neurons for the laminin isoforms. Neuronal differentiation, which was quantified as the neuron percentage (neuron count/total cell count), was efficient and similar to our previously published results (Lappalainen et al., 2010). Both the total cell and neuron counts were clearly highest on LN511 and the lowest on LN411. Difference between LN511 and LN411 occurs in the α-chain, and previous *in vivo* studies indicate the importance of the laminin α5-chain in CNS development (Miner et al., 1998) and the basement membrane of the hippocampus (Indyk et al., 2003). *In vitro* studies have also shown the superiority of LN511 over LN211 and LN411 as substrates for rodent primary neuron cultures (Fusaoka-Nishioka et al., 2011; Plantman et al., 2008). Our results are consistent with these findings, indicating that the laminin α5-chain has an important function in human CNS neurons. Despite the differences between rodent and human cells, as well as primary and stem cell-derived neurons, the same laminin chain or isoform efficiently supports neuronal growth *in vitro*.

Other commercially available substrates containing the α5-chain are the LN521 isoform and LN511-E8 fragment. Laminin isoforms −511 and −521 differ in the structures of their β chains, but the functional differences *in vivo* are not known (Rodin et al., 2014b). The LN511-E8 fragment is a truncated protein composed of the C-terminal regions of the α5, β1 and γ1 chains, including the integrin-binding site, but lacking some biological activities of the intact laminins. It is, however, easier and more efficient to produce the fragment than full-length laminin (Miyazaki et al., 2012b). LN521 and LN511-E8 have been used to differentiate hPSC-derived neurons (Miyazaki et al., 2012b; Rodin et al., 2014a) but a detailed comparison between the effects of the LN511, LN521, and LN511-E8 substrates on hPSC-derived neurons has not been performed. We studied this aspect and did not observe any differences between neuronal cultures on LN511 and LN521 in terms of cell attachment, survival, differentiation, or network formation. Minor decreases in the total cell and neuron counts were detected in cultures on LN511-E8 compared to cultures on LN511 and LN521. Collectively, hPSC-derived neurons behave similarly on all laminin substrates that contain the α5-chain.

In this study, gene expression profiles were analyzed in cells cultured on LN211, LN332, LN411 and LN511. In general, several genes related to human ECM and adhesion molecules were upregulated in cells cultured on all substrates compared to the suspension sample, suggesting for adhesion, neuronal migration and maturation processes following cell attachment to coated surfaces. The expression profiles in neurons cultured on LN411 and human laminin were the most strikingly divergent from the other groups, possibly as a consequence of the detected weak attachment and viability of neurons on these coating substrates. A more detailed comparison of cultures on LN511 and LN411, the most and the least supportive culture substrates, respectively, was performed to gain insights into the possible mechanisms underlying the detected laminin isoform preference. Multiple genes encoding ECM proteins (several collagen α1 chains, *LAMB3*, *FN1*, and *ECM1*) were either upregulated in the neuronal cultures on all coating substrates compared to the suspension sample or considerably upregulated in the LN511 cultures compared to the cultures on LN411. This result could indicate active ECM production by the human neurons under our culture conditions, as neuronal ECM production has previously been documented in different experimental designs using rodent primary neurons *in vitro* (Fudge and Mearow, 2013; Lander et al., 1998).

Integrins are important receptors for laminins that have specificities for certain laminin isoforms. LN511 has been identified as the most preferred ligand for several laminin-binding integrins, whereas LN411 only has modest affinity for two integrin receptors (Nishiuchi et al., 2006). *Integrin subunits αV*, *β4*, and *α1* were upregulated in cultures on LN511 compared to cultures on LN411, of which *αV* and *β4* form integrin receptors with reported specificity for LN511 (Nishiuchi et al., 2006; Sasaki and Timpl, 2001). *Integrin subunit α1* expression has been observed in the developing central and peripheral nervous systems and cultured rodent DRG neurons *in vitro* (Duband et al., 1992;

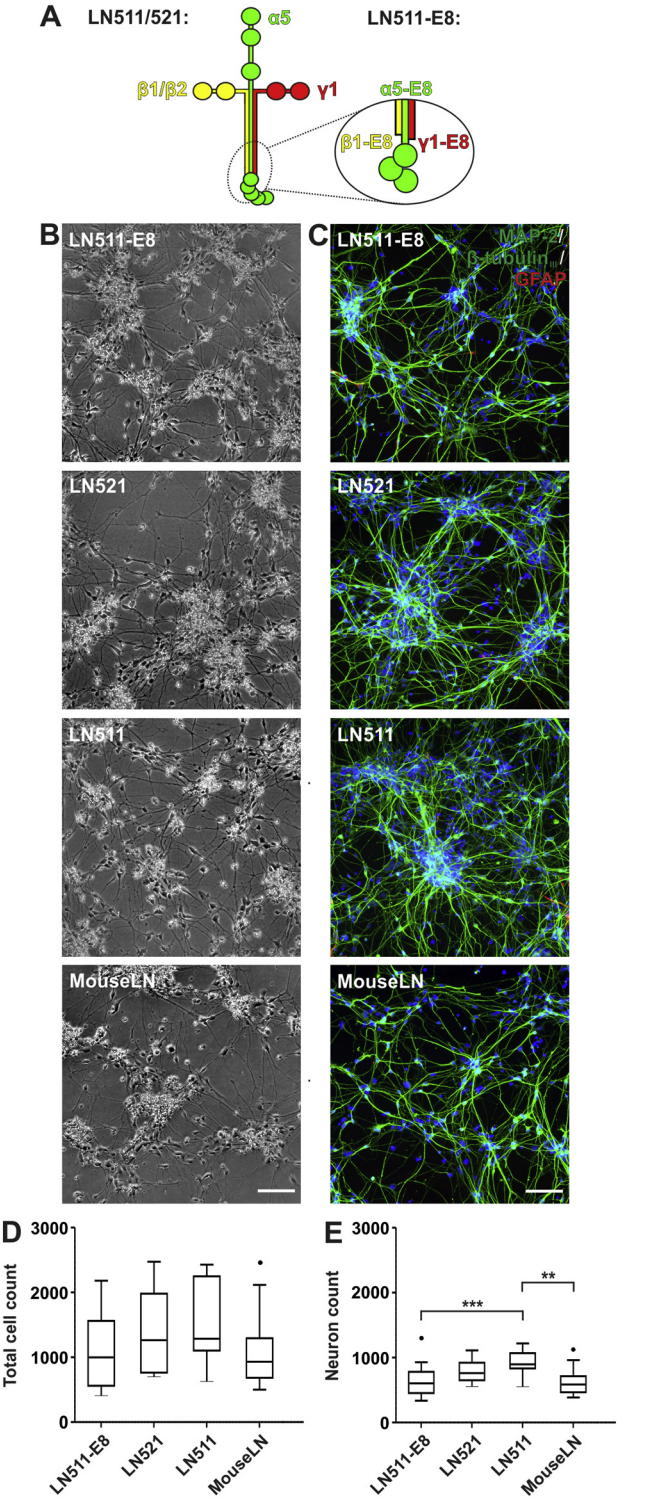

Fig. 5. Cell morphology and immunocytochemical characterization of hPSC-derived neurons on LN511-E8 and LN521. Protein expression of the neuronal markers MAP-2 and β-tubulin$_{III}$ were determined in hPSC-derived neurons cultured on LN511-E8, LN521, LN511, and mouse laminin for one week. A) Schematic representation of the intact LN511/LN521 and the LN511-E8 structures. B) Representative images of neuronal networks formed on different laminin substrates. Scale bar: 100 μm. C) Representative images of MAP-2/β-tubulin$_{III}$/GFAP-staining of hPSC-derived neurons on different laminin substrates. Scale bar: 100 μm. D) Total cell counts and E) neuron counts quantified in cultures on LN511-E8, LN521, LN511, and mouse laminin after one week. The data from three biological experiments presented as Tukey boxplots. Mann-Whitney *U* test (*$p \le 0.05$; **$p \le 0.01$; ***$p \le 0.005$). LN511, LN521, and LN511-E8 were first compared to mouse laminin, and then LN521 and LN511-E8 were compared to LN511.

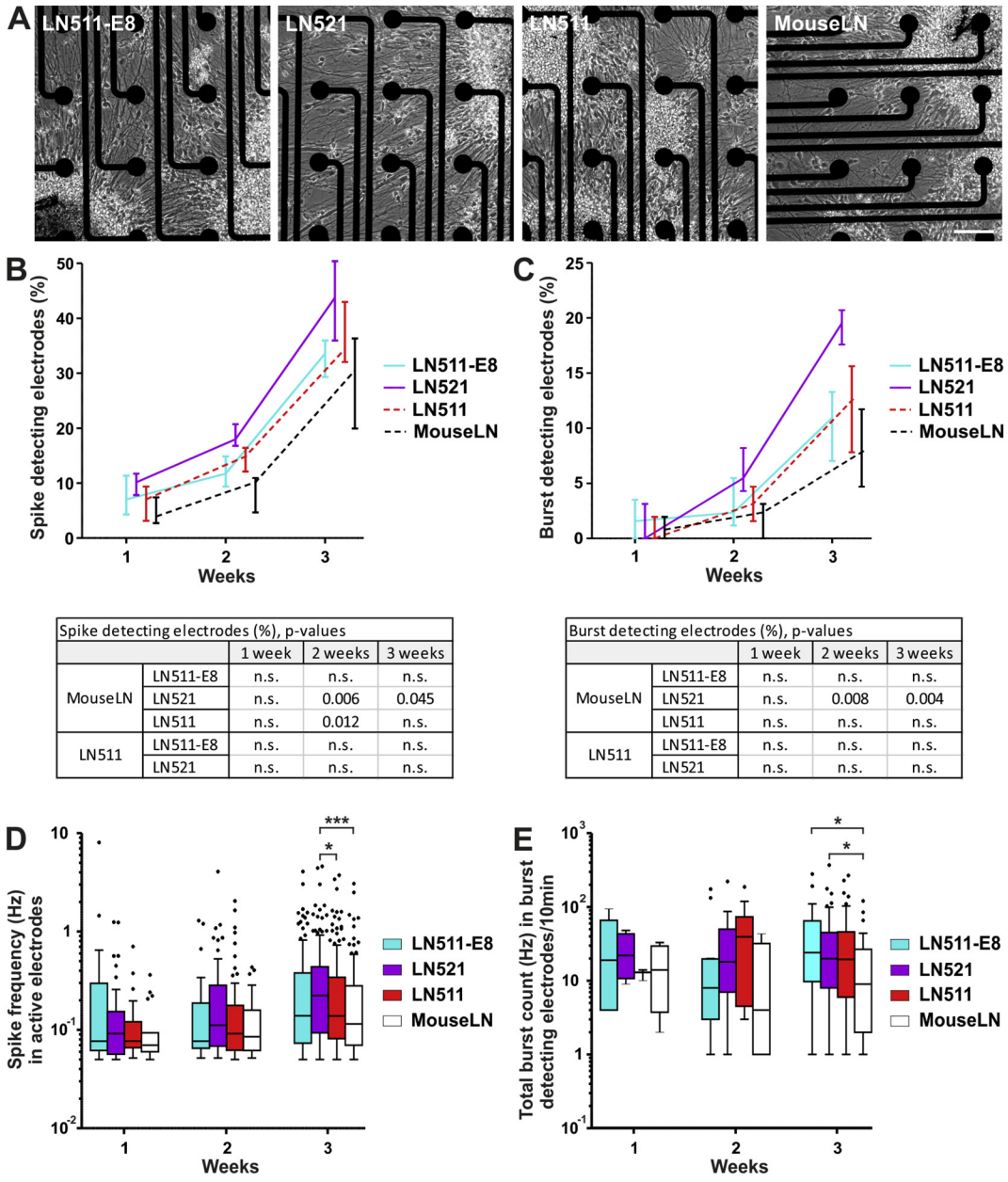

Spike detecting electrodes (%), p-values

		1 week	2 weeks	3 weeks
MouseLN	LN511-E8	n.s.	n.s.	n.s.
	LN521	n.s.	0.006	0.045
	LN511	n.s.	0.012	n.s.
LN511	LN511-E8	n.s.	n.s.	n.s.
	LN521	n.s.	n.s.	n.s.

Burst detecting electrodes (%), p-values

		1 week	2 weeks	3 weeks
MouseLN	LN511-E8	n.s.	n.s.	n.s.
	LN521	n.s.	0.008	0.004
	LN511	n.s.	n.s.	n.s.
LN511	LN511-E8	n.s.	n.s.	n.s.
	LN521	n.s.	n.s.	n.s.

Fig. 6. Development of spontaneous neuronal functionality in cultures on LN511-E8 and LN521. The hPSC-derived neurons were cultured on MEAs coated with LN511-E8, LN521, LN511, and mouse laminin for three weeks and electrophysiological activity was measured once a week. A) Representative phase contrast images of the neuronal networks formed on MEAs coated with different laminin substrates at the one week time point. Scale bar: 100 μm. B) Percentages of spike-detecting electrodes and C) burst-detecting electrodes after one, two, and three weeks. The results are presented as medians with interquartile ranges from six parallel cultures. D) Development of the spontaneous spiking frequency in active electrodes and E) total burst count in burst-detecting electrodes. The data from six parallel cultures presented as Tukey boxplots. Mann-Whitney *U* test (*$p \leq 0.05$; **$p \leq 0.01$; ***$p \leq 0.005$). LN511, LN521, and LN511-E8 were first compared to mouse laminin, and then LN521 and LN511-E8 were compared to LN511. Comparisons were performed at every time point.

Tomaselli et al., 1993). However, α1 integrins have not been previously identified as receptors of LN511 or LN411. Integrins can also bind other ECM proteins such as TGFBI and ICAM1. *ICAM1* and *TGFBI* were significantly upregulated in cultures on LN511 compared to cultures on LN411 in all cell lines included in this study. TGFBI contains RGD motif that interacts with αvβ3 integrin and modulates several integrin-mediated cellular functions in humans (Son et al., 2013). ICAM1 interacts with variety of receptors, including integrin subunits, αL, αM, and β2 (Etienne-Manneville et al., 1999). Thus, some integrin subunits can be upregulated in response to the expression of ECM proteins produced by the cultured cells. Proteinases are involved in breaking down the ECM (Werb, 1997), and the detected differences in the expression levels of *ADAMTS13* and *MMP10* between the LN511 and LN411 cultures could indicate variations in ECM remodeling in cultures on different laminin substrates. ECM proteins also bind growth factors, thereby regulating their bioavailability to the cells (Brizzi et al., 2012). Together, our results suggest that molecules involved in determining the laminin isoform preference in hPSC-derived neurons could be related to cell adhesion and ECM remodeling. Especially *ICAM1* and *TGFBI* could be potential targets for further studies investigating the mechanisms supporting growth and development of hPSC-derived neurons on LN511 *in vitro*.

Despite the crucial importance of spontaneous functionality and the functional development of neuronal networks *in vitro*, the effects of specific laminin isoforms on neuronal network activity have not previously been studied. When neuronal functionality was compared in cells on LN211, LN332, LN411, and LN511, the highest spontaneous network activity, in terms of spike- and burst-detecting electrode percentages, was detected in cultures on LN511. Previous studies with rodent primary

neurons have shown that the neuronal network density affects the functional characteristics of the network (Biffi et al., 2013; Wagenaar et al., 2006). A higher cell network density results in faster increase in the active electrode counts and bursting rates. Here, we showed that in addition to spreading evenly on the culture area and forming neuronal networks with highest density on LN511, the cultures showed the widest distribution of electrophysiologically active neurons. The comparison of the laminin α5 substrates LN511-E8, LN521, and LN511 revealed that there were no substantial differences in the development of functional neuronal networks, and these substrates were superior to the other laminin isoforms. Clear differences between the spontaneous spiking or bursting frequencies were not detected in the cultures on the different laminin substrates. This result suggests that laminin substrates have an important role in the initial adherence and basement membrane-like support for developing neuronal networks, but they do not affect specific characteristics of the neuronal network activity. However, only the most general parameters of electrophysiological activity are covered here; thus, this aspect should be addressed in more extensive electrophysiological studies.

Defined laminin substrates provide a more controlled cell culture environment for hPSC-derived neurons, which can be utilized for *in vitro* disease modeling, toxicological studies, and drug discovery. Recombinant isoforms are a relevant option for previously used, undefined, and heterogeneous human or mouse laminin. In addition, recombinant human laminin isoforms are also a promising approach for the production of hPSC-derived cells for regenerative medicine (Rodin et al., 2014a). Thus, hPSC culture and directed differentiation protocols utilizing same recombinant laminin isoforms or fragment(s) as cell culture substrates would be beneficial. Both LN511 and LN521 can support the self-renewal of hPSCs (Rodin et al., 2010; Rodin et al., 2014b), and patient-specific iPSCs can be derived, expanded, and further differentiated into dopaminergic neurons on LN521 (Lu et al., 2014). Our unpublished observations are similar in terms of efficient hPSC culturing on LN521, followed by neuronal differentiation in suspension culture (unpublished data). Efficient hPSC culturing (Miyazaki et al., 2012b; Rodin et al., 2014a) and further differentiation into dopaminergic neurons have also been reported on LN511-E8 (Doi et al., 2014; Nakagawa et al., 2014). However, conflicting results have been reported because LN511-E8 has shown to be an either more (Miyazaki et al., 2012b) or less (Rodin et al., 2014a) supportive culture substrate for hPSCs compared to the full-length LN511 isoform. Our results show that neuronal differentiation and maturation into functional neurons can be performed on LN511, LN521, and LN511-E8, but none of these laminin α5 substrates is superior.

5. Conclusions

In conclusion, we showed that according to the morphological, biochemical, and functional analyses, laminin α5 substrates provide efficient support and a defined *in vitro* environment for the generation of hPSC-derived neuronal networks, regardless of the used hPSC line. Our results provide novel insights into effects of different laminin isoforms on hPSC-derived neurons *in vitro* and can be further utilized for enhanced production of functional hPSC-derived neurons for research and clinical applications.

Supplementary data to this article can be found online at http://dx.doi.org/10.1016/j.scr.2017.09.002.

Acknowledgements

We thank statistician Heini Huhtala, M.Sc. and Laura Ylä-Outinen, Ph.D. for their assistance with statistical analyses and MEA. Tanja Paavilainen, M.Sc. and Teemu Ihalainen, Ph.D. are acknowledged for their assistance in image quantification and M.Sc. students Elina Haukkavaara and Emilia Hentinen for their assistance with immunocytochemical analyses. This work was financially supported by Doctoral Programme in Biomedicine and Biotechnology (BioMediTech, University of Tampere), the Finnish Funding Agency for Innovation (Tekes), and Finnish Cultural Foundation.

References

Barak, T., Kwan, K.Y., Louvi, A., Demirbilek, V., Saygi, S., Tuysuz, B., Choi, M., Boyaci, H., Doerschner, K., Zhu, Y., Kaymakcalan, H., Yilmaz, S., Bakircioglu, M., Caglayan, A.O., Ozturk, A.K., Yasuno, K., Brunken, W.J., Atalar, E., Yalcinkaya, C., Dincer, A., Bronen, R.A., Mane, S., Ozcelik, T., Lifton, R.P., Sestan, N., Bilguvar, K., Gunel, M., 2011. Recessive LAMC3 mutations cause malformations of occipital cortical development. Nat. Genet. 43, 590–594.

Barros, C.S., Franco, S.J., Muller, U., 2011. Extracellular matrix: functions in the nervous system. Cold Spring Harb. Perspect. Biol. 3, a005108.

Biffi, E., Regalia, G., Menegon, A., Ferrigno, G., Pedrocchi, A., 2013. The influence of neuronal density and maturation on network activity of hippocampal cell cultures: a methodological study. PLoS One 8, e83899.

Brizzi, M.F., Tarone, G., Defilippi, P., 2012. Extracellular matrix, integrins, and growth factors as tailors of the stem cell niche. Curr. Opin. Cell Biol. 24, 645–651.

Chun, S.J., Rasband, M.N., Sidman, R.L., Habib, A.A., Vartanian, T., 2003. Integrin-linked kinase is required for laminin-2-induced oligodendrocyte cell spreading and CNS myelination. J. Cell Biol. 163, 397–408.

Coles, E.G., Gammill, L.S., Miner, J.H., Bronner-Fraser, M., 2006. Abnormalities in neural crest cell migration in laminin alpha5 mutant mice. Dev. Biol. 289, 218–228.

Doi, D., Samata, B., Katsukawa, M., Kikuchi, T., Morizane, A., Ono, Y., Sekiguchi, K., Nakagawa, M., Parmar, M., Takahashi, J., 2014. Isolation of human induced pluripotent stem cell-derived dopaminergic progenitors by cell sorting for successful transplantation. Stem Cell Rep. 2, 337–350.

Domogatskaya, A., Rodin, S., Tryggvason, K., 2012. Functional diversity of laminins. Annu. Rev. Cell Dev. Biol. 28, 523–553.

Duband, J.L., Belkin, A.M., Syfrig, J., Thiery, J.P., Koteliansky, V.E., 1992. Expression of alpha 1 integrin, a laminin-collagen receptor, during myogenesis and neurogenesis in the avian embryo. Development 116, 585–600.

Etienne-Manneville, S., Chaverot, N., Strosberg, A.D., Couraud, P.O., 1999. ICAM-1-coupled signaling pathways in astrocytes converge to cyclic AMP response element-binding protein phosphorylation and TNF-alpha secretion. J. Immunol. 163, 668–674.

Fietz, S.A., Lachmann, R., Brandl, H., Kircher, M., Samusik, N., Schroder, R., Lakshmanaperumal, N., Henry, I., Vogt, J., Riehn, A., Distler, W., Nitsch, R., Enard, W., Paabo, S., Huttner, W.B., 2012. Transcriptomes of germinal zones of human and mouse fetal neocortex suggest a role of extracellular matrix in progenitor self-renewal. Proc. Natl. Acad. Sci. U. S. A. 109, 11836–11841.

Fudge, N.J., Mearow, K.M., 2013. Extracellular matrix-associated gene expression in adult sensory neuron populations cultured on a laminin substrate. BMC Neurosci. 14 (15-2202-14-15).

Fusaoka-Nishioka, E., Shimono, C., Taniguchi, Y., Togawa, A., Yamada, A., Inoue, E., Onodera, H., Sekiguchi, K., Imai, T., 2011. Differential effects of laminin isoforms on axon and dendrite development in hippocampal neurons. Neurosci. Res. 71, 421–426.

Halfter, W., Dong, S., Yip, Y.P., Willem, M., Mayer, U., 2002. A critical function of the pial basement membrane in cortical histogenesis. J. Neurosci. 22, 6029–6040.

Heikkilä, T.J., Yla-Outinen, L., Tanskanen, J.M., Lappalainen, R.S., Skottman, H., Suuronen, R., Mikkonen, J.E., Hyttinen, J.A., Narkilahti, S., 2009. Human embryonic stem cell-derived neuronal cells form spontaneously active neuronal networks in vitro. Exp. Neurol. 218, 109–116.

Indyk, J.A., Chen, Z.L., Tsirka, S.E., Strickland, S., 2003. Laminin chain expression suggests that laminin-10 is a major isoform in the mouse hippocampus and is degraded by the tissue plasminogen activator/plasmin protease cascade during excitotoxic injury. Neuroscience 116, 359–371.

Kapucu, F.E., Tanskanen, J.M., Mikkonen, J.E., Yla-Outinen, L., Narkilahti, S., Hyttinen, J.A., 2012. Burst analysis tool for developing neuronal networks exhibiting highly varying action potential dynamics. Front. Comput. Neurosci. 6, 38.

Lander, C., Zhang, H., Hockfield, S., 1998. Neurons produce a neuronal cell surface-associated chondroitin sulfate proteoglycan. J. Neurosci. 18, 174–183.

Lappalainen, R.S., Salomaki, M., Yla-Outinen, L., Heikkila, T.J., Hyttinen, J.A., Pihlajamaki, H., Suuronen, R., Skottman, H., Narkilahti, S., 2010. Similarly derived and cultured hESC lines show variation in their developmental potential towards neuronal cells in long-term culture. Regen. Med. 5, 749–762.

Lu, H.F., Chai, C., Lim, T.C., Leong, M.F., Lim, J.K., Gao, S., Lim, K.L., Wan, A.C., 2014. A defined xeno-free and feeder-free culture system for the derivation, expansion and direct differentiation of transgene-free patient-specific induced pluripotent stem cells. Biomaterials 35, 2816–2826.

Miner, J.H., Cunningham, J., Sanes, J.R., 1998. Roles for laminin in embryogenesis: exencephaly, syndactyly, and placentopathy in mice lacking the laminin alpha5 chain. J. Cell Biol. 143, 1713–1723.

Miyazaki, T., Futaki, S., Hasegawa, K., Kawasaki, M., Sanzen, N., Hayashi, M., Kawase, E., Sekiguchi, K., Nakatsuji, N., Suemori, H., 2008. Recombinant human laminin isoforms can support the undifferentiated growth of human embryonic stem cells. Biochem. Biophys. Res. Commun. 375, 27–32.

Miyazaki, T., Futaki, S., Suemori, H., Taniguchi, Y., Yamada, M., Kawasaki, M., Hayashi, M., Kumagai, H., Nakatsuji, N., Sekiguchi, K., Kawase, E., 2012a. Laminin E8 fragments support efficient adhesion and expansion of dissociated human pluripotent stem cells. Nat. Commun. 3, 1236.

Miyazaki, T., Futaki, S., Suemori, H., Taniguchi, Y., Yamada, M., Kawasaki, M., Hayashi, M., Kumagai, H., Nakatsuji, N., Sekiguchi, K., Kawase, E., 2012b. Laminin E8 fragments support efficient adhesion and expansion of dissociated human pluripotent stem cells. Nat. Commun. 3, 1236.

Nakagawa, M., Taniguchi, Y., Senda, S., Takizawa, N., Ichisaka, T., Asano, K., Morizane, A., Doi, D., Takahashi, J., Nishizawa, M., Yoshida, Y., Toyoda, T., Osafune, K., Sekiguchi, K., Yamanaka, S., 2014. A novel efficient feeder-free culture system for the derivation of human induced pluripotent stem cells. Sci. Rep. 4, 3594.

Nishiuchi, R., Takagi, J., Hayashi, M., Ido, H., Yagi, Y., Sanzen, N., Tsuji, T., Yamada, M., Sekiguchi, K., 2006. Ligand-binding specificities of laminin-binding integrins: a comprehensive survey of laminin-integrin interactions using recombinant alpha3beta1, alpha6beta1, alpha7beta1 and alpha6beta4 integrins. Matrix Biol. 25, 189–197.

Ojala, M., Prajapati, C., Polonen, R.P., Rajala, K., Pekkanen-Mattila, M., Rasku, J., Larsson, K., Aalto-Setala, K., 2016. Mutation-specific phenotypes in hiPSC-derived cardiomyocytes carrying either myosin-binding protein C or alpha-tropomyosin mutation for hypertrophic cardiomyopathy. Stem Cells Int. 2016, 1684792.

Plantman, S., Patarroyo, M., Fried, K., Domogatskaya, A., Tryggvason, K., Hammarberg, H., Cullheim, S., 2008. Integrin-laminin interactions controlling neurite outgrowth from adult DRG neurons in vitro. Mol. Cell. Neurosci. 39, 50–62.

Radner, S., Banos, C., Bachay, G., Li, Y.N., Hunter, D.D., Brunken, W.J., 2013. K.T. Yee, beta2 and gamma3 laminins are critical cortical basement membrane components: ablation of Lamb2 and Lamc3 genes disrupts cortical lamination and produces dysplasia. Dev. Neurobiol. 73, 209–229.

Rodin, S., Domogatskaya, A., Strom, S., Hansson, E.M., Chien, K.R., Inzunza, J., Hovatta, O., Tryggvason, K., 2010. Long-term self-renewal of human pluripotent stem cells on human recombinant laminin-511. Nat. Biotechnol. 28, 611–615.

Rodin, S., Antonsson, L., Hovatta, O., Tryggvason, K., 2014a. Monolayer culturing and cloning of human pluripotent stem cells on laminin-521-based matrices under xeno-free and chemically defined conditions. Nat. Protoc. 9, 2354–2368.

Rodin, S., Antonsson, L., Niaudet, C., Simonson, O.E., Salmela, E., Hansson, E.M., Domogatskaya, A., Xiao, Z., Damdimopoulou, P., Sheikhi, M., Inzunza, J., Nilsson, A.S., Baker, D., Kuiper, R., Sun, Y., Blennow, E., Nordenskjold, M., Grinnemo, K.H., Kere, J., Betsholtz, C., Hovatta, O., Tryggvason, K., 2014b. Clonal culturing of human embryonic stem cells on laminin-521/E-cadherin matrix in defined and xeno-free environment. Nat. Commun. 5, 3195.

Sasaki, T., Timpl, R., 2001. Domain IVa of laminin alpha5 chain is cell-adhesive and binds beta1 and alphaVbeta3 integrins through Arg-Gly-Asp. FEBS Lett. 509, 181–185.

Simon-Assmann, P., Orend, G., Mammadova-Bach, E., Spenle, C., Lefebvre, O., 2011. Role of laminins in physiological and pathological angiogenesis. Int. J. Dev. Biol. 55, 455–465.

Sixt, M., Engelhardt, B., Pausch, F., Hallmann, R., Wendler, O., Sorokin, L.M., 2001. Endothelial cell laminin isoforms, laminins 8 and 10, play decisive roles in T cell recruitment across the blood-brain barrier in experimental autoimmune encephalomyelitis. J. Cell Biol. 153, 933–946.

Skottman, H., 2010. Derivation and characterization of three new human embryonic stem cell lines in Finland. In Vitro Cell. Dev. Biol. Anim. 46, 206–209.

Son, H.N., Nam, J.O., Kim, S., Kim, I.S., 2013. Multiple FAS1 domains and the RGD motif of TGFBI act cooperatively to bind alphavbeta3 integrin, leading to anti-angiogenic and anti-tumor effects. Biochim. Biophys. Acta 1833, 2378–2388.

Toivonen, S., Ojala, M., Hyysalo, A., Ilmarinen, T., Rajala, K., Pekkanen-Mattila, M., Aanismaa, R., Lundin, K., Palgi, J., Weltner, J., Trokovic, R., Silvennoinen, O., Skottman, H., Narkilahti, S., Aalto-Setala, K., Otonkoski, T., 2013. Comparative analysis of targeted differentiation of human induced pluripotent stem cells (hiPSCs) and human embryonic stem cells reveals variability associated with incomplete transgene silencing in retrovirally derived hiPSC lines. Stem Cells Transl. Med. 2, 83–93.

Tomaselli, K.J., Doherty, P., Emmett, C.J., Damsky, C.H., Walsh, F.S., Reichardt, L.F., 1993. Expression of beta 1 integrins in sensory neurons of the dorsal root ganglion and their functions in neurite outgrowth on two laminin isoforms. J. Neurosci. 13, 4880–4888.

Wagenaar, D.A., Pine, J., Potter, S.M., 2006. An extremely rich repertoire of bursting patterns during the development of cortical cultures. BMC Neurosci. 7, 11.

Werb, Z., 1997. ECM and cell surface proteolysis: regulating cellular ecology. Cell 91, 439–442.

Yla-Outinen, L., Heikkila, J., Skottman, H., Suuronen, R., Aanismaa, R., Narkilahti, S., 2010. Human cell-based micro electrode array platform for studying neurotoxicity. Front. Neuroeng. 3. http://dx.doi.org/10.3389/fneng.2010.00111 (eCollection 2010).

Ylä-Outinen, L., Joki, T., Varjola, M., Skottman, H., Narkilahti, S., 2014. Three-dimensional growth matrix for human embryonic stem cell-derived neuronal cells. J. Tissue Eng. Regen. Med. 8, 186–194.